Solvent and structural effects in tautomeric 3-cyano-4-(substituted phenyl)-6-phenyl-2(1H)-pyridones: Experimental and quantum chemical study

ARTICLE *in* STRUCTURAL CHEMISTRY · FEBRUARY 2014

Impact Factor: 1.84 · DOI: 10.1007/s11224-014-0401-y

7 AUTHORS, INCLUDING:

Ismail Ajaj
University of Belgrade
6 PUBLICATIONS **12** CITATIONS
SEE PROFILE

Jasmina S. Markovski
The Polytechnic School , Ira A. Fulton Scho…
11 PUBLICATIONS **17** CITATIONS
SEE PROFILE

Milos Milcic
University of Belgrade
38 PUBLICATIONS **242** CITATIONS
SEE PROFILE

Struct Chem
DOI 10.1007/s11224-014-0401-y

ORIGINAL RESEARCH

Solvent and structural effects in tautomeric 3-cyano-4-(substituted phenyl)-6-phenyl-2(1*H*)-pyridones: experimental and quantum chemical study

Ismail Ajaj · Jasmina Markovski · Jelena Marković · Maja Jovanović · Miloš Milčić · Fathi Assaleh · Aleksandar Marinković

Received: 25 July 2013 / Accepted: 15 January 2014

Abstract The tautomeric equilibria between 2-pyridone and 2-hydroxypyridine forms of methoxy, chloro, and nitro derivatives of 3-cyano-4-(2-, 3-, and 4-substituted phenyl)-6-phenyl-2(1*H*)-pyridones were evaluated from UV/Vis spectral data. Linear solvation energy relationships of Kamlet–Taft and Catalán-rationalized solvent have influence on tautomeric equilibria. Transmission of substituent effect was analyzed by the Hammett equation. Quantum chemical calculations were performed by density functional theory (B3LYP). The experimental data were interpreted with the aid of time-dependent density functional method. Electron density distribution was analyzed by Bader's analysis. It was found that substituents of different electronic properties change the extent of conjugation, and affect intramolecular charge transfer character. Theoretical calculations and experimental results gave insight into the influence of the molecular conformation on the transmission of substituent effects, as well as on contribution of different solvent–solute interactions.

Keywords Tautomerism · Solvent effects · Substituent effects · UV–Vis absorption spectroscopy · DFT

Electronic supplementary material The online version of this article (doi:10.1007/s11224-014-0401-y) contains supplementary material, which is available to authorized users.

I. Ajaj · J. Marković · A. Marinković
Faculty of Technology and Metallurgy, University of Belgrade, Karnegijeva 4, 11120 Belgrade, Serbia
e-mail: marinko@tmf.bg.ac.rs

J. Markovski (✉)
Vinča Institute, University of Belgrade, 11000 Belgrade, Serbia
e-mail: jasmina.markovski@tmf.bg.ac.rs

M. Jovanović · M. Milčić
Faculty of Chemistry, University of Belgrade, Studentski trg 3–5, 11000 Belgrade, Serbia

F. Assaleh
Faculty of Pharmacy, Zawia University, P.O. Box 16168, Zawia, Libya

Introduction

Pyridines represent an important class of compounds due to the different physiological properties of their derivatives. Among them, 2(1*H*)-pyridones have not only the biological importance but also a significant industrial application. 3-Cyano-2(1*H*)-pyridones have cardiotonic activity. On the other hand, 3-cyano-2(1*H*)-pyridones are used in production of paints, pigments, fuels, and additives [1].

2(1*H*)-Pyridones comprise –NH–C(=O)– group, which makes them susceptible to the **PY/HP** (lactam/lactim) tautomerism. This type of tautomerism has been the subject of studies in many fields of chemistry and biochemistry. Such studies were used in the explanation of tautomeric equilibria of nucleobases, cytosine [2, 3], thymine [4, 5], and uracil [6, 7]; rationalization of structures, properties, and reactivities in heterocyclic chemistry [8], concepts and probes of aromaticity [8], measures of intrinsic stabilities *vs* solvent effects [9], mechanisms of enzymatic catalysis and receptor interactions [8], and possibly even mutations during DNA and RNA replications [8].

Tautomeric equilibrium between **PY** and **HP** forms depends on the environment: self-association, solvation, dimerization, ion binding, and substituents present at pyridone nuclei [9]. IR, UV/Vis [9, 10], NMR [11], and mass spectrometric studies confirmed that **PY** predominates in the gas phase under equilibrium conditions [12], and in inert matrices. In nonpolar solvents, both tautomers

Published online: 02 February 2014

exist in comparable amounts; while the tautomeric equilibrium is shifted toward **PY** form in aqueous solutions, polar solvents, as well as in the crystalline state [13, 14]. It is also well known that solvent polarity and hydrogen-bonding ability significantly affect the tautomeric equilibrium. Situation in solution is further complicated due to possible self-association where three types of dimmers: **PY–PY**, **HP–HP** and mixed **PY–HP** one can be formed. The presence of dimmers in solution decreases as temperature increases, or it could be dissociated by the addition of solvents with strong HBA/HBD abilities, which break intermolecular hydrogen bonds in dimmers [13–16].

In this study, linear solvation energy relationship (LSER), linear free energy relationship (LFER) correlations, and **quantum-chemical calculations of** 3-cyano-4-(2-, 3-, and 4-substituted phenyl)-6-phenyl-2(1*H*)-pyridones with 2-(**1**), 3-(**2**), and 4-methoxy (**3**); 2-(**4**), 3-(**5**) and 4-chloro (**6**); and 2-(**7**), 3-(**8**) and 4-nitro (**9**) substituent (Fig. 1), were performed. The most widely used LSER model—applied for the quantification of the effect of solvent dipolarity/polarizability and hydrogen-bonding interactions—introduced by Kamlet–Taft [17], is given by Eq. (1):

$$v = v_0 + s\pi^* + b\beta + a\alpha \tag{1}$$

where v values are the absorption frequency maxima; π^* is an index of the solvent dipolarity/-polarizabilty; β is a measure of the solvent hydrogen bonding acceptor (HBA) basicity; α is a measure of the solvent hydrogen bonding donor (HBD) acidity; and v_0 is the regression value corresponding to cyclohexane as reference solvent. Kamlet–Taft solvent parameters are given in Supplementary material, Table S1 [17, 18]. The regression coefficients s, b, and a in Eq. (1) reflect relative susceptibilities of the absorption maxima to the solvent parameters.

More elaborated LSER model uses Catalán solvent parameters scale [19], *i.e.*, Eq. (2) which qualitatively and quantitatively interprets the effect of solvent dipolarity, polarizability, and solvent–solute hydrogen bonding interactions:

$$v = v_0 + a\mathrm{SA} + b\mathrm{SB} + c\mathrm{SP} + d\mathrm{SdP} \tag{2}$$

where SA, SB, SP, and SdP characterize solvent acidity, basicity, polarizability, and dipolarity, respectively (Table S2). The regression coefficients *a–d* describe the sensitivity of the absorption maxima to different types of the solvent–solute interactions. The transmission of substituent effects was studied using Hammett equation Eq. (3):

$$v = \rho\sigma + h \tag{3}$$

where v are the substituent-dependent values, *i.e.*, the absorption frequency maxima, ρ is the proportionality constant (reaction constant) which reflects sensitivity of the measured values v to substituent effects, σ is the appropriate substituent constant (Table S3), and h is the intercept (*i.e.*, describes the unsubstituted member of the series) [20].

The UV/Vis spectroscopic data were analyzed by LSER and LFER models to evaluate the tautomeric equilibria and the intramolecular charge transfer (ICT) in the investigated set of compounds (**1–9**). The resolution of the individual bands in UV–Vis spectra [21] was based on various assumptions and approximations [22], and was applied for the evaluation of the state of tautomeric equilibria. LSER study was helpful in explaining multiple solvent–solute interactions.

Geometries of compounds were optimized by DFT calculations. The estimation of the transition energy was obtained from time-dependent density functional theory (TD-DFT) calculation which systematically includes all possible solvent–solute interactions. TD-DFT was

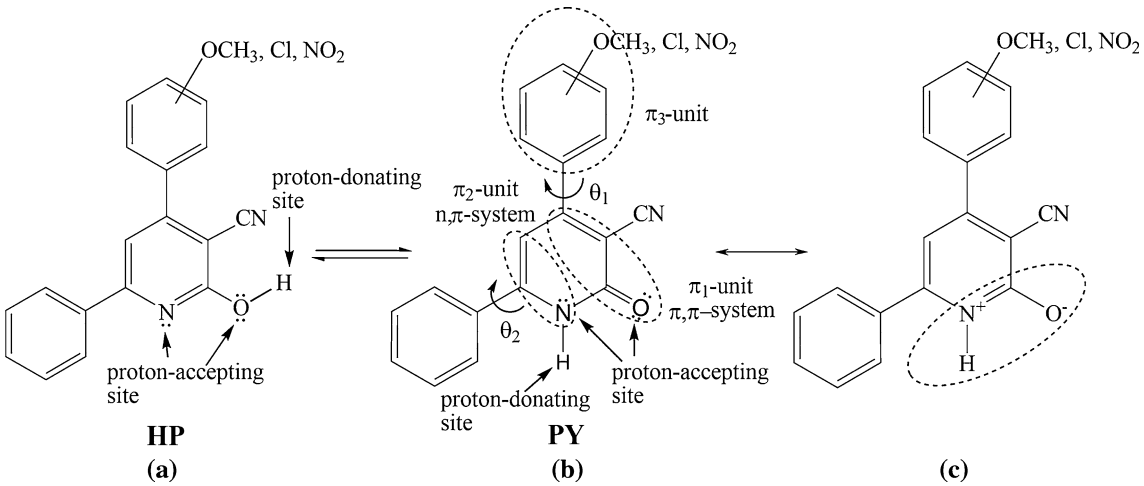

Fig. 1 Tautomeric equilibria of **HP a**, **PY b**, and zwitter-ion structure **c** of investigated compounds

successfully applied for the description of solvated organic molecules with a possibility of estimation of electronic density transfer from a donor to an acceptor group [23], and for study of the influences of molecular geometry on ICT [24]. The successfulness of DFT method was proven by the study of simple and water-assisted tautomerism in amidrazones [25], and for the explanation of prototropic tautomerism and microsolvation in antitumor drugs [26]. The transmission of substituent effects was additionally discussed in relation to the geometry of molecules and the charge distribution, as obtained by DFT calculation and Bader's analysis.

Experimental

Materials

All the used materials and solvents (UV spectrophotometric grade) were obtained commercially (Fluka and Sigma-Aldrich), and used without purification.

Synthesis of 2(1H)-pyridones

Synthesis of methoxy, nitro and chloro derivatives of 3-cyano-4-(2-, 3-, and 4-substituted phenyl)-6-phenyl-2(1*H*)-pyridones was described in the previous study [27].

Equipment

FTIR spectra were recorded in transmission mode on BOMEM (Hartmann & Braun) instrument, MB series in the form of KBr pellets. The purity of the obtained compounds was confirmed by elemental analysis.

^{1}H and ^{13}C NMR characterizations were performed on a Varian Gemini 2000 (200/50 MHz) instrument at 25 °C. Chemical shifts (δ) were reported in part per million (ppm) relative to tetramethylsilane ($\delta_H = 0$ ppm) in ^{1}H NMR, and to dimethyl sulfoxide ($\delta_C = 39.5$ ppm) in ^{13}C NMR, using the residual solvent peak as a reference standard. 2D Nuclear Overhauser effect spectroscopy (NOESY), Heteronuclear Multiple Bond Correlation (HMBC), and Heteronuclear single quantum coherence spectroscopy (HSQC) spectra were recorded on a Bruker Avance 500 spectrometer (500/125 MHz) equipped with inverse detection triple resonance 5-mm probe (TXI). Standard pulse sequences were used for 2D spectra [27].

The UV absorption spectra were recorded on UV–Vis Shimadzu 1700A spectro-photometer at different conditions, *e.g.,* variable temperature and concentration, as well as solvent mixtures, which were expected to have effect on the tautomer ratio and the extent of dimerization: concentration was changed in the range from 1.00×10^{-4} to 1.00×10^{-7} mol dm^{-3}, and at temperatures of 25, 35, 45, and 55 ± 0.1 °C. The constant $K_T = [\mathbf{PY}]/[\mathbf{HP}]$ represents proportion of the area of the corresponding tautomeric form.

Molecular geometry optimization and theoretical absorption spectra calculation

The ground state geometries of compounds **1**–**9** were fully optimized with DFT method (more specifically the Becke three-parameter exchange functional (B3) and the Lee–Yang–Parr correlation functional (LYP)) with 6-311G(d,p) basis set without symmetry constrain, and with default tight convergence criteria. Global minima were found for each molecule. Harmonic vibrational frequencies have been evaluated at the same level to confirm the nature of the stationary points found (to confirm that optimized geometry corresponding to minimum that has only real frequencies), and to account for the zero point vibrational energy (ZPVE) correction. Solvents have been simulated with standard static isodensity surface-polarized continuum model (IPCM). Theoretical absorption spectra of both tautomeric forms were calculated in gas phase, ethanol, tetrahydrofuran, acetonitrile and dimethylsulfoxide with TD-DFT method. The frontier molecular orbital energies: E_{HOMO} for the highest occupied molecular orbital (HOMO) and E_{LUMO} for the lowest unoccupied molecular orbital (LUMO) and HOMO–LUMO energy gaps (E_{gap}) were also calculated using the same methods. All the calculations were done with Gaussian03 software [28]. The Bader's analysis were done on charge density grid using the program "Bader" [29]. The ground-state and excited-state electron densities were calculated on ground-state- optimized geometries using B3LYP/6-311(d,p) method. Density difference maps were plotted as difference between electron densities of the excited state and the ground state, in program gOpenMol [30].

Regression analysis

The correlation analysis was carried out using Microsoft Excel software, considering 95 % confidence level. The quality of correlations was evaluated by the correlation coefficient (R), standard error of the estimate (Sd), and Fisher's test of significance (F).

Results and discussion

Resolution of UV spectra

2(1*H*)-pyridones exist in a solution as the equilibrium of tautomeric and/or dimer forms [16, 31], and these phenomena have significant influences on their physicochemical properties. The tautomeric equilibrium is affected

by the factors inherent to studied molecules, geometries, and substituent effects, while others are associated to solvent properties like polarity, stabilization of the charges in the solvation sphere and from alteration of a solute's electronic structure in the ground and excited states due to both short- and long-range interactions with surrounding solvent molecules [32, 33].

A study of the mechanism of proton-transfer and state of equilibria in solution is an interesting and complex phenomenon, which needs careful analysis to avoid misinterpretation of the results obtained. Different spectroscopic techniques were used for studying solvent–solute interactions and state of tautomeric equilibria. Slow proton exchange allows for the observation of distinct signals in ^{1}H NMR spectra, which could be used for qualitative and quantitative determinations of each tautomeric form [34]. When the proton exchange is fast compared with NMR timescale, in the NMR spectrum of a tautomeric mixture only one, average, signal can be observed. Fast proton exchange limited applicability of NMR spectroscopy for the study of prototropic equilibria in the case of studied 2(1*H*)-pyridones. Therefore, we used advantages of the UV/Vis absorption spectroscopy in the following: tautomeric forms have different spectral characteristics, and the tautomeric equilibrium is influenced by various external factors like environment (solvent), substituent effect, acidity, temperature, etc. Consequently, examination of the tautomeric equilibria, solvatochromism, and transmission of substituent effects through appropriate tautomeric forms of compounds **1–9** were performed by analyzing UV/Vis spectra. Resolution of individual bands in UV–Vis spectra was best described with the pure Gauss or with the mixed Gauss–Lorentz functions [21]. Spectral properties determination was based on various assumptions and approximations [22].

In general, tautomeric equilibrium is shifted toward more dipolar **PY** form with increasing solvent polarity due to the larger contribution of the charge-separated mesomeric form (Fig. 1c) [9], while the opposite is true for nonpolar solvents.

Absorption spectra of the investigated compounds were recorded in 17 solvents. It was found that the spectra consist of two overlapped bands in the region of 300–500 nm. Mutual ratio of the bands depends on both the substituent effects and the solvent properties. Influences of solvent–solute interactions on molecular associations (dimer formation) have been thoroughly investigated [13–16]. To study the appearance of dimerization and its influence on spectroscopic properties, the UV/Vis spectra of 2(1*H*)-pyridones were recorded at different concentrations and temperatures (Fig. S1). The results showed no effect on K_T at concentrations less than 1×10^{-5} mol dm^{-3}, indicating no monomer content rising upon dilution. Therefore, the presence of dimeric forms did not affect UV spectra at low solute concentration. All UV/Vis spectra were recorded at the concentration of 1×10^{-5} mol dm^{-3}. Also, negligible influences of temperature changes were observed (Fig. S1) [35–37].

The absorption maxima of both **PY** (higher wavelength energy band) and **HP** forms (lower one) in the set of selected solvents are given in Tables 1 and 2, respectively. The characteristic absorption spectra in ethanol, THF, and NMF are shown in Fig. 2 and Fig. S2 in Supplementary Material, respectively.

The spectra consisting of overlapped bands were analyzed by a stepwise procedure, whereby estimations of both tautomerization constants and individual spectra of the tautomers were obtained from experimental data and DFT calculation. Because of the shape of spectra shown in Fig. 2, and the observation that overlapped bands were present in a UV/Vis spectra, we performed detailed analysis of the structure of spectral bands. The resolution of the individual bands was a complex task due to high extent of the overlapping of absorption bands and difficulties related to estimation of their number. Derivative spectroscopy was a very useful tool in determining the number and the approximate position of the absorption bands.

In the first step, we determined the approximate number of bands and the position of each band, by applying second and fourth derivative spectroscopy [38]. In the second step, the initial approximation of the band intensities and band widths and assignment to the appropriate tautomeric form were performed. The final refinement is performed by simultaneous resolution of the whole set of spectra according to the literature procedures described in references [25, 38, 39]. Results are exemplified in Figs. S3 and S4, and the results obtained are given in Tables 1 and 2. Such methodology provides differentiation without loss of the terminal spectral points [40].

The absorption maxima shifts showed low dependence with respect to both solvent and substituent effects (Tables 1, 2), and the lower values of ν_{max} were found for electron-acceptor-substituted compounds (the lowest for compound **9**). The ν_{max} shifts are influenced by solvent–solute nonspecific (dipolarity/polarizability) and specific (HBA/HBD) interactions. The solvent hydrogen-bonding ability plays a specific role in solvation of appropriate tautomeric forms: HBD solvent effect contributes to better stabilization of the oxo form (**PY**), whereas HBA stabilizes better the hydroxy form (**HP**) [41]; in this way, their balanced contribution cause state of tautomeric equilibria.

LSER analysis of UV data

The influences of various types of solvent–solute interactions on the absorption maxima shifts were interpreted by

Table 1 Absorption frequencies of the **PY** form in selected solvents

Solvent/compound	$\nu_{max} \times 10^{-3}$ (cm^{-1})								
	0[a]	1-PY	2-PY	3-PY	4-PY	5-PY	6-PY	7-PY	8-PY	9-PY
Methanol	27.55	27.78	27.53	27.03	27.53	27.43	27.23	27.47	27.11	26.84
Ethanol	27.47	27.64	27.23	26.74	27.49	27.41	27.03	27.19	26.87	26.75
1-Propanol	27.25	27.22	26.95	26.69	27.47	27.13	27.03	27.38	26.75	26.78
2-Propanol	27.32	27.13	26.83	26.69	27.20	27.25	27.17	27.25	26.88	26.52
1-Butanol	27.25	27.05	26.75	26.67	27.46	27.40	27.32	27.20	26.81	26.48
2-Butanol	27.28	26.97	26.79	26.96	27.46	27.26	27.08	27.23	26.68	26.57
1,4-Dioxane (dioxane)	26.78	26.55	26.41	26.42	26.99	27.06	26.74	26.42	26.70	26.56
Ethyl acetate (EtAc[b])	26.95	26.55	26.47	26.46	26.82	26.88	26.95	26.82	26.52	26.27
Tetrahydrofuran (THF)	26.74	26.50	26.54	26.41	26.66	26.04	26.71	26.27	25.80	25.80
Acetonitrile (AcN)	26.87	27.40	27.01	26.55	27.12	26.99	26.81	26.79	26.67	25.64
Acetone	27.08	27.19	26.87	27.04	27.01	26.88	26.74	26.90	26.52	26.25
Dimethyl sulfoxide (DMSO)	26.65	26.35	26.16	26.02	26.53	26.49	26.38	27.12	26.11	24.60
N,N-Dimethylformamide (DMF)	26.60	26.28	26.03	25.97	26.64	26.52	26.38	26.94	26.18	24.45
N,N-Dimethylacetamide (DMAc)	26.52	26.32	26.11	26.11	26.71	26.45	26.45	27.23	26.05	24.04
N-Methylformamide (NMF)	27.51	27.35	26.98	27.30	27.08	27.06	26.94	27.43	26.50	26.05
Dichloromethane (DCM)	27.30	27.11	27.17	26.98	27.08	27.16	26.95	27.23	26.79	26.48
Chloroform (Chl)	27.41	27.70	27.35	27.56	27.43	27.32	27.17	27.16	26.68	26.51

[a] Unsubstituted compounds

[b] Abbreviations taken from www.chemnetbase.com

Table 2 Absorption frequencies of the **HP** form in selected solvents

Solvent/compound	$\nu_{max} \times 10^{-3}$ (cm^{-1})								
	0[a]	1-HP	2-HP	3-HP	4-HP	5-HP	6-HP	7-HP	8-HP	9-HP
Methanol	30.31	29.91	29.91	29.99	29.99	29.73	29.75	30.25	29.21	29.13
Ethanol	29.99	29.82	29.51	30.03	29.35	29.56	29.80	29.78	28.93	28.52
1-Propanol	29.39	29.79	29.64	30.00	29.76	29.70	29.13	29.57	28.67	28.67
2-Propanol	29.68	30.13	29.75	30.18	29.23	29.63	29.25	29.56	29.01	28.99
1-Butanol	30.17	29.81	29.43	30.47	29.18	29.13	29.20	30.06	28.51	28.94
2-Butanol	30.18	29.83	29.68	30.43	29.13	29.67	29.43	30.13	29.60	29.51
Dioxane	29.88	29.80	29.51	30.53	29.31	29.80	29.62	29.58	29.82	29.63
EtAc	30.13	29.63	29.62	30.73	29.40	29.43	29.31	30.25	29.37	29.15
THF	30.47	29.99	29.93	30.63	29.80	29.56	28.67	30.08	29.28	29.50
AcN	27.13	29.03	28.80	30.30	29.00	29.10	28.17	27.05	27.98	28.12
Acetone	29.05	29.32	29.00	30.21	28.80	28.93	28.95	28.98	28.90	28.21
DMSO	28.31	28.98	28.31	29.75	27.63	29.09	28.90	27.73	28.13	25.20
DMF	28.70	29.27	28.64	29.81	27.91	29.13	28.95	28.80	27.50	25.33
DMAc	27.36	29.65	29.00	30.13	28.52	29.12	28.10	28.01	27.45	27.31
NMF	28.77	29.57	28.98	30.52	28.51	28.91	29.57	28.67	27.64	29.81
DCM	28.15	28.67	28.50	29.90	28.42	28.71	28.42	27.95	28.37	28.03
Chl	29.21	29.07	29.52	30.21	30.05	29.30	29.07	28.92	28.72	28.71

[a] Unsubstituted compound [27]

means of the LSER models of Kamlet–Taft (Eq. 1) and Catalán (Eq. 2). The Kamlet–Taft and the Catalan parameters [18–20], given in Tables S1 and S2, were used for the evaluation of the solute–solvent interactions and the solvatochromic shifts of the UV/Vis absorption maxima of the investigated compounds. In general, the correlation results support conclusions about relation between the solvent–solute interactions and the state of tautomeric

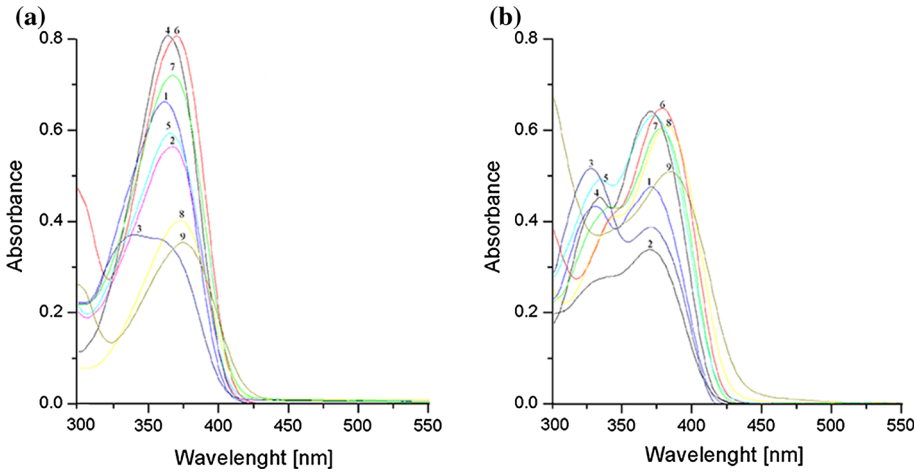

Fig. 2 Absorption spectra of compounds **1**–**9** in **a** ethanol and **b** THF

equilibria. The values of the correlation coefficients, obtained according to Kamlet–Taft and the Catalán equations, are illustrated in Tables 3 and 4 for the **PY** form, and Tables S4 and S5 for **HP** form, respectively. The contribution percentages of the nonspecific (P_π) and the specific solvent/solute interactions (P_β and P_α) are given in Tables S6 and S7, respectively.

The correlation results helped us to evaluate the contribution of the each type of solvent–solute interactions on the spectral shift change of the appropriate tautomeric form. The positive value of the coefficient *a*, obtained for the **PY** form, indicates better stabilization of the molecule in the ground state (Table 3). Oppositely, negative sign of the coefficient *a*, obtained for the **HP** form (Table S4; except comps. **4** and **6**), indicates batochromic shift in relation to increased contribution of the HBD effect. It means that proton-accepting capabilities of both pyridine nitrogen and hydroxyl group in the **HP** form contribute in moderate extent to the solute stabilization in excited state (Table S4).

Negative signs of the coefficients *s* and *b*, obtained in correlations for the **PY** form (Table 3), indicate a batochromic shift of the absorption maxima with the increasing contribution of solvent dipolarity/polarizability and hydrogen-accepting capability. The largest values of coefficients *s* and *b* of the **PY** form were found in compound **9** (Table 3). It means that the most effective transmission of the substituent effect, *i.e.,* electron-accepting ability of the nitro group, from *para*-position to the amide NH group increase dipolarity/polarizability and hydrogen-bonding capability of compound **9**. In the case of the compounds in the **HP** forms, nonspecific solvent effect is the main contributing factor influencing batochromic shift, while specific solvent effects showed a lower and complex influence on solvatochromism of the investigated compounds (Table S4). Nonspecific solvent effect is more pronounced in compounds in the **HP** form, compared with the **PY** form, and the largest effect was obtained for nitro-substituted compounds **7**–**9**.

The correlation results, obtained following Eq. (2), implied that the solvent dipolarity is the principal factor influencing the batochromic shift (Table 4).

Quantitative separation of the nonspecific solvent effect (coefficient s; Tables 3, S4) on polarizability and dipolarity term (coefficients *c* and *d*, Tables 4, S5), showed high significance of the solvent dipolarity on stabilization of the excited state in both forms. High values of coefficient *d* and lower values of coefficient *c* obtained for all compounds in the **HP** form (Table S5), indicate pronounced influence of solvent dipolarity and less polarizability effects on ν_{max} change. This means that strong electron-withdrawing character of the nitro group causes high extent of π-electron delocalization which contributes to larger dipolarity and π-electron polarizability of compunds in the **HP** form. This could not be applied for compounds in the **PY** form where the most pronounced nonspecific solvent effect was noticed only for compound **9**. It means that contribution of zwitter-ionic structure (Fig. 1c) in an overall resonance hybrid of compound **9** in the **PY** form causes increased molecule dipolarity.

Solvent hydrogen-bonding interactions have moderate–to –low contribution on the absorption maxima shift and preferentially acts through hydrogen-bonding with the hydroxyl and the pyridine aza groups of the solutes in the **HP** form (Table S5). Significant number of compounds show negligible values and complex influence of specific solvent effects on solvatochromism of the investigated compounds (Table S5). Negative values of the coefficient *b* indicate higher stabilization of the excited state in **PY** form, while the opposite is true for HBD solvent effect (Table 4).

The comparison of the correlation results obtained for unsubstituted compound in the **PY** form indicates low contribution of nonspecific solvent effect (Table 3). Similar results, negligible *d* and moderate value of coefficient *c*, were obtained according to Catalán Eq. (2) (Table 4). Such

Table 3 The results of the correlation analysis for **PY** tautomer obtained according to Kamlet–Taft Eq. (1)

Comp.	$v_0 \times 10^{-3}$ (cm^{-1})	$s \times 10^{-3}$ (cm^{-1})	$a \times 10^{-3}$ (cm^{-1})	$b \times 10^{-3}$ (cm^{-1})	R^a	Sd[b]	F^c	Solvent excluded from correlation
0[d]	27.20 ± 0.16	–0.26 ± 0.18	0.86 ± 0.09	–0.50 ± 0.08	0.96	0.09	66.71	NMF, acetone, dioxane
1-PY	27.66 ± 0.15	–0.66 ± 0.19	0.73 ± 0.10	–0.30 ± 0.11	0.95	0.12	41.08	–
2-PY	27.35 ± 0.10	–0.51 ± 0.13	0.81 ± 0.07	–0.54 ± 0.07	0.98	0.08	95.16	–
3-PY	27.54 ± 0.13	–0.59 ± 0.16	1.02 ± 0.09	–0.37 ± 0.10	0.98	0.10	88.12	–
4-PY	27.53 ± 0.12	–0.65 ± 0.15	0.58 ± 0.08	–0.29 ± 0.08	0.96	0.09	50.09	–
5-PY	27.43 ± 0.11	–0.59 ± 0.14	0.72 ± 0.07	–0.47 ± 0.08	0.97	0.08	73.13	–
6-PY	27.35 ± 0.14	–0.70 ± 0.18	0.54 ± 0.09	–0.32 ± 0.10	0.94	0.11	33.11	–
7-PY	26.88 ± 0.26	–[e]	0.71 ± 0.10	–0.22 ± 0.14	0.93	0.10	20.25	DMSO, DMF, DMAc
8-PY	27.13 ± 0.12	–0.56 ± 0.14	0.62 ± 0.08	–0.62 ± 0.11	0.96	0.09	40.05	DMF, Chl
9-PY	28.39 ± 0.59	–3.09 ± 0.74	1.10 ± 0.36	–1.35 ± 0.37	0.92	0.39	22.73	NMF

[a] Correlation coefficient

[b] Standard deviation

[c] Fisher test of significance

[d] Unsubstituted compound [27]

[e] Negligible values with high standard errors

Table 4 The results of the correlation analysis for **PY** tautomers obtained according to Catalán Eq. (2)

Comp.	$v_0 \times 10^{-3}$ (cm^{-1})	$a \times 10^{-3}$ (cm^{-1})	$b \times 10^{-3}$ (cm^{-1})	$c \times 10^{-3}$ (cm^{-1})	$d \times 10^{-3}$ (cm^{-1})	R	Sd	F	Solvent excluded from correlation[a]
0[b]	28.13 ± 0.66	1.57 ± 0.32	–0.61 ± 0.20	–1.01 ± 0.31	–[c]	0.92	0.16	13.34	Acetone, dioxane
1-PY	29.50 ± 0.44	0.88 ± 0.21	–[c]	–0.33 ± 0.17	–3.02 ± 0.62	0.95	0.12	37.2	Chl
2-PY	28.81 ± 0.60	1.41 ± 0.29	–0.82 ± 0.21	–0.81 ± 0.30	–1.34 ± 0.79	0.93	0.16	15.7	2-Butanol, dioxane
3-PY	29.26 ± 0.69	1.82 ± 0.34	–0.58 ± 0.23	–0.55 ± 0.26	–2.09 ± 0.91	0.93	0.18	18.2	–
4-PY	28.48 ± 0.60	1.67 ± 0.42	–0.68 ± 0.28	–0.49 ± 0.23	–1.10 ± 0.83	0.90	0.16	9.19	Methanol, Chl
5-PY	28.66 ± 0.53	1.33 ± 0.26	–0.71 ± 0.19	–0.74 ± 0.20	–1.28 ± 0.70	0.93	0.14	17.1	2-Butanol
6-PY	28.83 ± 0.43	0.86 ± 0.21	–0.35 ± 0.14	–1.27 ± 0.21	–1.21 ± 0.57	0.95	0.11	22.4	Dioxane
7-PY	25.73 ± 0.70	1.22 ± 0.22	–[c]	–[c]	1.49 ± 0.86	0.92	0.11	10.8	DMSO, DMAc, DCM
8-PY	28.48 ± 0.32	0.95 ± 0.15	–0.43 ± 0.11	–0.52 ± 0.12	–1.97 ± 0.41	0.97	0.08	33.7	DMAc, DCM
9-PY	32.78 ± 1.57	2.21 ± 0.76	–1.38 ± 0.53	–2.72 ± 0.59	–6.05 ± 2.07	0.92	0.42	14.6	–

[a] No available literature data of solvent parameters for NMF; excluded from Catalán correlation

[b] Unsubstituted compound [27]

[c] Negligible values with high standard errors

result strongly indicates low contribution of zwitter-ionic structure c) (Fig. 1) to overall resonance hybrid of this compound in the **PY** form. Solvent dipolarity and polarizability are dominant effects contributing to higher stabilization of excited state of unsubstituted compound in the **HP** form (Tables S4, S5). Larger dipolarity and π-electron mobility of the **HP** form iare mainly the consequence of appropriate molecular geometry, which enable larger extent of π-electron conjugative transfer. Introduction of electron-donating substituents causes decreases of π-electron mobility, *i.e.*, decreases of contribution of dipolarity and polarizability effects. Oppositely, introduction of electron-accepting substituents, from chloro to nitro, causes significant increases of coefficients c and d (Table S5; except comps. **6** and **8**).

In order to examine the influence of HBD solvent effect on the state of tautomeric equilibria, UV/Vis spectra of some compounds were recorded in a different set of solvent mixtures. Representative examples of UV spectra of compound **3,** recorded in a mixture of THF/NMF, are shown on Fig. 3a. The second derivative of the spectra are presented in Fig. 3b. An example of the K_T evaluation is given in Fig. S4, and the determined K_T values are: $K_T = 0.46$ (100 % THF); $K_T = 0.53$ (70 % THF); $K_T = 0.82$ (50 % THF); $K_T = 0.96$ (30 % THF); and $K_T = 1.40$ (10 % THF). the obtained results showed

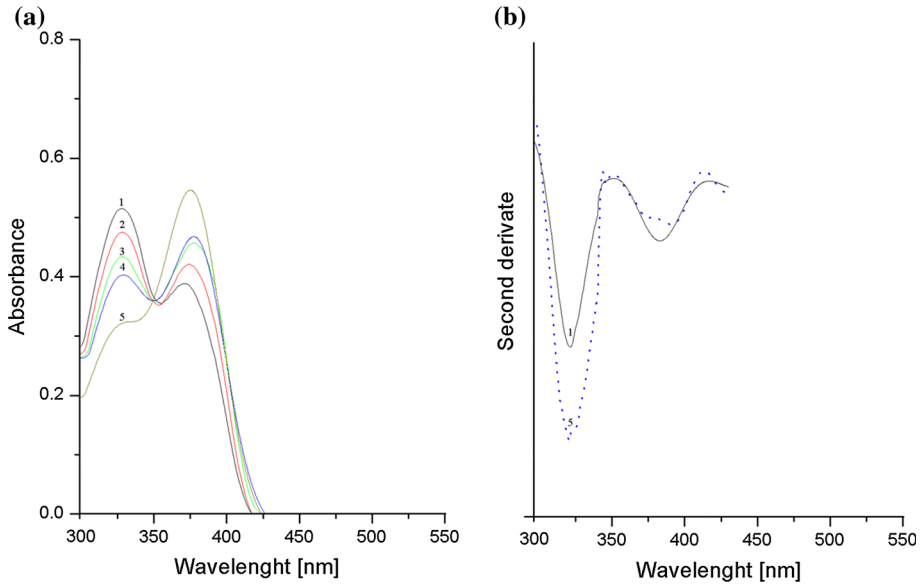

Fig. 3 Absorption spectra of comp. **3** in a different v/v ratios of THF/NMF: **a** 100 %; **2** 70 %; **3** 50 %; **4** 30 %; **5**, and 10 % THF; **b** Second derivate of spectra **1** and **5**

appropriate relation between **PY/HP** tautomer and the contribution of appropriate solvent effects [25].

It is noticeable that tautomeric forms exist in different ratios in appropriate solvent mixture. Increasing proportion of protic solvent, *i.e.*, increasing of hydrogen-bonding capability of solvent mixture, causes increase of K_T value. Solvation phenomena refer to the interaction between the dissolved molecule and the solvents, which leads to the stabilization of the system by formation of solvation shells. In a binary mixtures of solvents, a solute could form different types of preferential interactions with surrounding solvent molecules in different extent. This is in accordance with the fact that higher HBD ability of solvent mixture shift equilibrium toward the lactam form [9]. Also, this is an example how adjustment of HBD/HBA properties of solvent mixture could control the state of tautomeric equilibria.

The success of the quantification and interpretation of solvent effects on the position of the absorption maxima of the investigated molecules (Fig. 4) was evaluated by plotting the calculated frequency (ν_{calc}), obtained by Catalán parameter set, versus the measured frequency (ν_{exp}) ($R = 0.95$, Sd = 0.18, $F = 1295.6$).

According to the described method, K_T values of the investigated compounds in all used solvents were determined, and the results are presented in Table 5.

The changes in the K_t values (Table 5) are the consequence of the contribution of both solvent effects as well as the nature of the substituent present. Balanced contribution of protic solvent effects on K_T (increased contribution of HBD effect) causes shift of the tautomeric equilibria to the **PY** form (higher K_t values); opposite is true for aprotic solvents, *i.e.*, solvent with increased dipolarity/polarizability

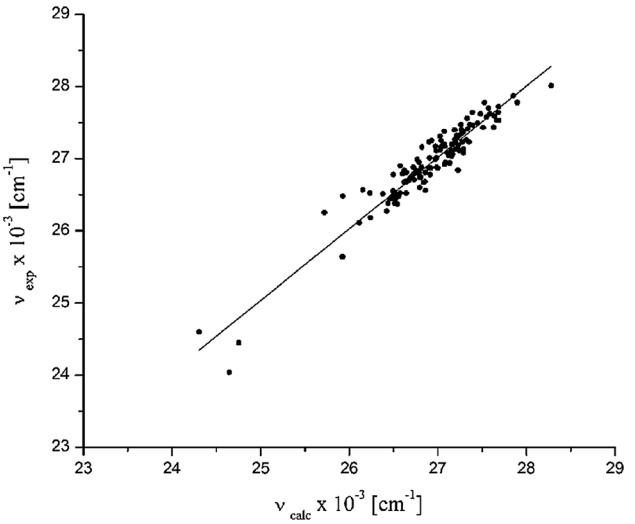

Fig. 4 The plot of ν_{exp} versus ν_{calc}

and proton-accepting capability (lower K_t values). It could be postulated that such behavior is a consequence in the differences in conjugational ability of the π-electron densities through localized or delocalized π-electronic systems of the appropriate tautomeric forms.

LFER analysis of UV data

A comprehensive analysis of substituent effects on absorption spectra of the investigated molecules, by using LFER principles in the form of the Hammett equation (Eq. 3), was performed. The correlation results for **PY** and **HP** forms are given in Tables 6 and S8, respectively.

Table 5 Equilibrum constants K_T in selected solvents

Solvent	Relative permittivity[a]	K_T/compound								
		1	2	3	4	5	6	7	8	9
Methanol	32.66	1.42	1.26	1.41	1.35	1.21	1.27	1.33	1.25	1.40
Ethanol	24.55	1.08	1.17	2.00	1.06	1.05	1.17	1.46	1.09	1.28
1-Propanol	20.45	1.17	1.18	1.24	1.22	1.31	1.28	1.37	1.29	1.36
2-Propanol	19.92	1.23	1.19	1.05	1.03	1.17	1.21	1.05	1.07	1.11
1-Butanol	17.51	1.05	1.14	1.12	1.75	1.81	1.79	1.06	1.11	1.13
2-Butanol	16.56	1.19	1.80	1.99	1.93	1.89	1.91	1.32	1.45	1.49
Dioxane	2.21	0.76	0.79	0.58	0.80	0.73	0.61	0.63	0.59	0.60
EtAc	6.02	0.78	0.71	0.79	0.75	0.69	0.77	0.73	0.89	0.67
THF	7.58	0.66	0.65	0.46	0.82	0.65	0.67	0.61	0.69	0.59
ACN	35.94	0.63	0.79	0.70	0.65	0.81	0.72	0.73	0.77	0.81
Acetone	20.56	0.75	0.88	0.71	0.73	0.88	0.79	0.78	0.81	0.80
DMSO	46.45	0.72	0.55	0.41	0.68	0.61	0.59	0.79	0.75	0.69
DMF	36.71	0.70	0.51	0.34	0.65	0.60	0.58	0.74	0.72	0.67
DMAc	37.78	0.60	0.77	0.36	0.56	0.63	0.59	0.67	0.70	0.65
NMF	182.40	1.20	1.18	1.80	1.36	1.38	1.95	1.38	1.66	1.93
DCM	8.93	1.13	1.07	1.01	1.11	1.09	1.07	1.18	1.12	1.10
Chl	4.89	1.02	1.21	1.36	1.03	1.20	1.29	1.10	1.12	1.15

[a] Ref Reichardt [13]

Table 6 Regression fits according to Eq. (3) for the **PY** form of investigated compounds

Solvent/ compound	$v_0 \times 10^{-3}$ (cm^{-1})	$\rho \times 10^{-3}$ (cm^{-1})	R	Sd	F	$v_0 \times 10^{-3}$ (cm^{-1})	$\rho \times 10^{-3}$ (cm^{-1})	R	Sd	F
	2, 3, 5, 6, 8, 9					**1, 4, 7**				
Methanol	27.67 ± 0.08	–0.97 ± 0.17	0.94	0.15	31.9	27.75 ± 0.08	−0.23 ± 0.09	0.93	0.09	6.2
Ethanol	27.50 ± 0.11	–0.93 ± 0.24	0.93	0.20	35.5	27.67 ± 0.01	−0.45 ± 0.01	0.99	0.01	7871
1-Propanol	27.40 ± 0.06	–0.88 ± 0.12	0.96	0.10	54.1	27.60 ± 0.05	−0.23 ± 0.08	0.95	0.05	8.9
2-Propanol	27.49 ± 0.07	–1.04 ± 0.15	0.96	0.13	45.9	27.57 ± 0.13	−0.38 ± 0.09	0.91	0.17	7.6
1-Butanol	27.45 ± 0.01	–0.94 ± 0.24	0.93	0.21	32.0	27.61 ± 0.01	−0.39 ± 0.01	0.99	0.01	1058.1
2-Butanol	27.39 ± 0.07	–0.97 ± 0.15	0.96	0.13	43.5	27.63 ± 0.02	−0.39 ± 0.03	0.99	0.02	174.3
EtAc	27.00 ± 0.07	–0.73 ± 0.15	0.92	0.13	22.4	27.29 ± 0.01	−0.43 ± 0.01	0.99	0.01	7871
THF	26.87 ± 0.19	–0.94 ± 0.40	0.91	0.15	30.2	26.98 ± 0.05	−0.20 ± 0.07	0.94	0.05	7.8
Acetone	26.93 ± 0.07	–0.66 ± 0.16	0.91	0.14	17.9	27.17 ± 0.06	−0.28 ± 0.09	0.95	0.06	9.3
DCM	27.19 ± 0.09	–0.67 ± 0.19	0.92	0.16	22.1	27.07 ± 0.05	−0.13 ± 0.07	0.92	0.06	5.9
	2, 3, 6, 8, 9					**1, 4, 5, 7**				
Dioxane	26.96 ± 0.05	–0.48 ± 0.09	0.94	0.08	24.5	27.21 ± 0.01	−0.36 ± 0.02	0.99	0.01	275.5
Chl	27.37 ± 0.05	–1.01 ± 0.10	0.98	0.09	95.9	27.63 ± 0.09	−0.49 ± 0.16	0.91	0.12	8.9
AcN	27.10 ± 0.22	–1.27 ± 0.44	0.92	0.40	18.2	27.34 ± 0.10	−0.56 ± 0.17	0.92	0.12	10.8
	2, 3, 6, 8, 9					**1, 4, 5**				
NMF	27.09 ± 0.09	–1.06 ± 0.19	0.95	0.17	29.65	27.40 ± 0.04	−0.85 ± 0.12	0.99	0.03	49.2
	2, 3, 6, 9					**1, 4, 5, 7, 8**				
DMSO	26.48 ± 0.25	–2.08 ± 0.58	0.93	0.41	13.3	26.75 ± 0.20	0.43 ± 0.33	0.91	0.20	7.5
DMF	26.44 ± 0.27	–2.18 ± 0.63	0.94	0.37	12.1	26.56 ± 0.30	0.10 ± 0.46	0.91	0.35	5.5
DMAc	26.52 ± 0.37	–2.68 ± 0.86	0.91	0.64	9.8	26.58 ± 0.22	0.55 ± 0.35	0.92	0.27	6.7

The correlation results (Table 6), classified in the four sets of solvents and two groups (columns) of substituent-dependent correlation results, reflect the balanced interplay of solvent and substituent effects on absorption maxima shifts. The introduction of both electron-donating and electron-withdrawing substituents contributes to positive solvatochromism in all solvents, except for compounds **1**, **4**, **5**, **7**, and **8** in DMSO, DMF, and DMAc. Good correlation results were obtained in all solvents.

In the first set of protic solvent (comps. **2**, **3**, **5**, **6**, **8**, and **9**), as well as the second and third sets of solvents (comps. **2**, **3**, **6**, **8**, and **9**), similar correlation slopes were observed. Somewhat higher values was noticed for solvents, which shows increased HBD property: Chl, AcN, and NMF. These results indicate that solvent effects—dipolarity/polarizability, HBD and HBA abilities—cause appropriate sensitivity of the position of absorption maxima (ν_{max}) to substituent effect. In the last set of aprotic solvents (DMSO, DMF, and DMAc), the highest sensitivity of ν_{max} to substituent effect was found. Exceptionally higher values of correlation slope, found for compounds **2, 3, 6**, and **9** in DMSO, DMF, and DMAc, indicate the utmost significance of the solvent dipolarity/polarizability and proton-accepting capabilities to higher stabilization of excited state of these compounds.

Lower susceptibility of the ν_{max} shifts to the electronic substituent effects was found for *ortho*-substituted 2(1*H*)-pyridones, *i.e*., compounds **1**, **4**, and **7** (first set of solvents), for compounds **1**, **4**, **5**, and **7** (second set), and for compounds **1**, **4**, **5**, **7,** and **8** (fourth set; lower value was found for DMF). Significantly higher slope ($\rho = -0.85$) was noticed for NMF. These results showed specific influences of the *ortho*-substituents on the shift of absorption maxima. It is generally assumed that *ortho*-effects include electronic, steric, and anisotropic factors [27]. Electronic and steric effects exert significant influence on solvatochromism. The electronic effect is not necessarily transmitted exclusively by polar (inductive) and π-electron delocalization (resonance) mechanisms, but could also be transmitted through space. Steric effect includes electronic density shift, bond length and bond angle change, and effect due to size of the *ortho*-substituent.

Results of LFER study clearly show higher stabilization of the **PY** form in the excited state, observed for compounds **2**, **3**, **6**, and **9** in DMSO, DMF, and DMAc. Higher sensitivities of their absorption frequencies to substituent effects in these solvents might be explained in following way: at high relative permittivity of surrounding medium, the energy necessary to bring about charge separation in the excited state is relatively small, which gives rise to a higher susceptibility to electronic substituent effects. Highly dipolar aprotic solvents (DMSO, DMF, and DMAc) behave as poor anion solvators, while they usually better stabilize larger and more dispersible positive charges. The electronic systems of the investigated 2(1*H*)-pyridones, considering their *non*-planarity [as obtained from DFT calculation (Tables S9–S11)], could be more susceptible to the substituent influence. Study of the transmission of substituent electronic effects through defined π-resonance units (Fig. 1b) showed that they behave either as isolated or conjugated fragments, and depend on substitution pattern under consideration [27].

Correlation obtained for the data derived in NMF indicates the significance of both HBD and nonspecific solvent properties of NMF. Higher slope obtained for compounds **1**, **4** ,and **5** (second column) indicate that an appropriate balance of substituent and solvent effect may effectively contribute at different extents in the ground and in the excited states to the stabilization of solute. The complex influences of both solvent and substituent effects on UV/Vis absorption maxima of the **HP** forms (Table S8), confirmed such conclusions, contributing to higher sensitivity and larger stabilization of excited state.

DFT, TD-DFT and Bader's analysis. Evaluation of electronic transition, and charge density change

An additional analysis of solvent and substituent effects on absorption frequencies, tautomeric equilibria, and conformational changes of the studied compounds necessitated quantum-chemical calculations, *i.e*., geometry optimization and charge density analysis. Geometry optimization of the investigated molecules was performed by the use of B3LYP functional with 6-311G(d,p) basis set. The most stable conformations of compounds **1–3** in both **PY** and **HP** forms are presented in Fig. S5. Detailed information on elements of optimized geometries of compounds **1–9** are given in Tables S9–S11. Molecular geometries parameters of the **PY** and **HP** forms are fairly similar, and despite this, the relationship between structural elements and solvatohromism is not fully consistent. Theoretical absorption spectra of both tautomeric forms, *i.e.,* the absorption frequencies ν_{max}, calculated in gas phase, ethanol, THF, AcN, and DMSO with TD-DFT method are given in Tables S12 and S13.

The feature of the greatest interest in the ground state of investigated compounds is represented by the values of torsion angle θ_1 (Fig. 1b), which are, among other factors, significantly influenced by the magnitude of substituent effects (Tables S9–S11). It is generally accepted that higher planarity of molecule, *i.e*., lower torsional angle, induces red shift in the absorption spectra. In the investigated molecules, these values are somewhat larger for the **PY** than for the **HP** form, which means that transmission of the electronic substituent effects, mainly resonance interaction, is more suppressed in the **PY** form. Somewhat larger differences of θ_1 was noticed for compound **7** (Table S11: 39.10 for **7-PY** and 22.74 for **7-HP**), indicating significance of *ortho*-effect, *i.e.,* vicinity of the substituent which exert large polar (inductive/field) and steric effects. It also explained the significance of the through-space field effect [27], which causes appropriate perturbation of π-electron density of the pyridone ring.

The results shown in Tables S9–S11 indicate that bond lengths of the **PY** and **HP** forms are obviously different, while lower differences in bond lengths between *ortho*-, *meta*- and *para*-substituted compounds could be observed. In the **PY** form, low influences of the substituent electronic effects are observed, while in the **HP** form, a well-defined alternation could be noticed. Appropriate values of bond distances are in the frame of statistical errors, and thus they are not suitable for evaluation purpose. In general, the bond lengths of the carbonyl groups become longer, while the bond length of C14–C23 (Fig S7) gets shorter, and the deviation from the planarity (expressed in term of torsional angle θ_1) decreases with the increasing electron-donating ability of the substituent. A decrease in the C14–C23 bond length, which is a bridging bond between π_1- and π_3-units, indicates a greater extent of the extended π,π-delocalization. The results are opposite for the electron-acceptor-substituted compounds **7–9** (Table S11). The common polarization of carbonyl groups is suppressed, and the slight decrease of the bond length was observed (Table S11). In general, an electron-acceptor withdraws electron density from pyridone ring, causing decrease of the extent of π,π-conjugation in enone system (π_1-unit), and simultaneously exerts enhancement of n,π-conjugation in π_2-unit (Fig. 1). The largest contribution of solvent effects to stabilization of solvated molecules in ground state was obtained in polar aprotic solvents, AcN and DMSO, and ethanol exerts somewhat lower influence, while lowest stabilization was found in THF (Tables S9–S11).

Mechanisms of electronic excitations and the electron density distribution in ground and excited states were studied by calculation of HOMO/LUMO energies (E_{HOMO}/E_{LUMO}) and E_{gap} values (Tables S14–S16, and Fig. S6). In general, a lower E_{gap} values were observed for all compounds in the **PY** form, and the lowest values were found for nitro-substituted compounds in both **PY** and **HP** forms. Small influences of *ortho*-substitution on increased E_{gap} could be observed for compounds **1–6** in the **HP** form (Tables S14 and S15). Low effects on E_{gap} changes, in both forms of compounds **1–6** (Tables S14 and S15), were observed by inclusion of implicit solvent model. For compounds **4–6** (Table S15), the substituent effects influence on E_{gap} changes showed similar trend as for compounds **1–3** (Table S14). Higher values of E_{gap} was found for compounds **7–9** in **HP** form, and the highest values for compounds **7** and **8** were noticed (Table S16). Additional discussion on TD-DFT results is given in Supplementary material (pages 12 and 13).

In order to obtain data on electronic density distribution, the Bader's analysis was performed. Difference of atomic charges in the excited and in the ground state (Δ_{charge}) for appropriate atoms, as well as calculated changes in overall electron density of molecules are given in Tables S17-S20. Atom and ring numbering used in Bader's analysis is given in Fig. S7.

According to the results shown in Tables S17–S20 and Figs 5, S8, and S9, it could be observed that in both **HP** and **PY** forms of the methoxy- and nitro-substituted compounds (**1–3** and **7–9**, respectively), ICT processes can be clearly observed. In methoxy-substituted compounds electron density was transferred from the-substituted phenyl to pyridine and unsubstituted phenyl moieties (Fig. 5). According to the character of the ICT processes, molecules can be divided in two groups:

The first group includes **HP** forms (**1-HP**, **2-HP**, and **3-HP**) along with **2-PY** compound. In these molecules, significant ICT process can be observed;-substituted rings lose from –0.77 to –0.88 electrons. The largest part of the

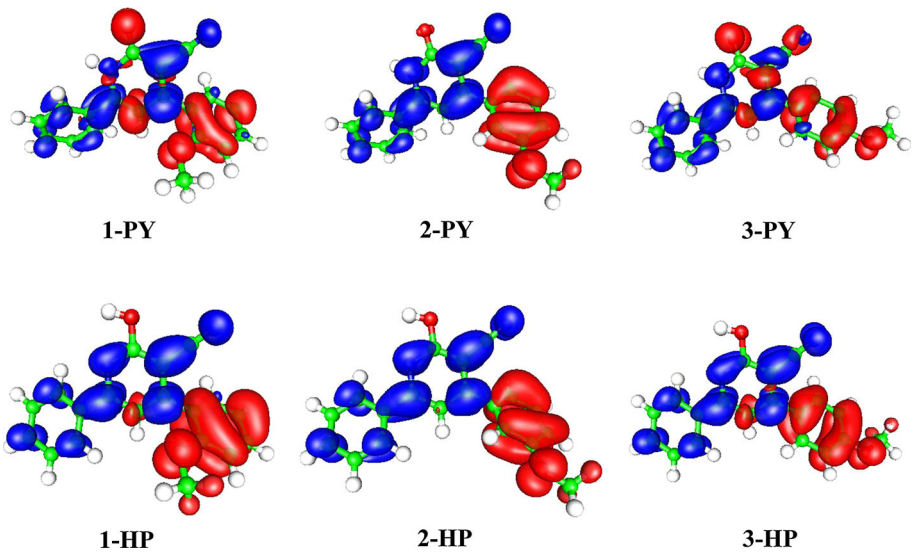

Fig. 5 ICT processes, *i.e.*, charge transfer of electron density from ground state (*red*) to excited state (*blue*) in both **PY** and **PH** forms of compounds **1–3** (Color figure online)

charge is transferred to the pyridine ring (Δ_{charge} for the pyridine ring varies from 0.58 to 0.70), *i.e.*, mostly to the ring carbon atoms (C12, C14 ,and C15).

In the second group, which includes compounds **1-PY** and **3-PY**, ICT process is less pronounced. The calculation showed that substituted phenyl moieties of **1-PY** and **3-PY** compounds lose –0.31 and –0.36 electrons, while pyridine ring receives 0.16 and 0.15 electrons, respectively. Along with this, O21 atom of the pyridone ring loses a significant amount of charge (Δ_{charge}): –0.1315 for **1-PY** and –0.1527 for **3-PY**). In the first group of compounds, charge difference of this atom appeared negligible. Observed charge transfer can be compared with resonance effect for compounds **1-PY** and **3-PY**, bearing *ortho* and *para* MeO-substituent. It should be noted that in all *methox*y-substituted compounds, charge differences between ground and excited states on unsubstituted phenyl ring are roughly similar (from 0.15 to 0.21).

Compounds with the chloro substituent (**4**–**6**) showed negligible ICT between the substituted ring and the other two ones. Charge density changes for substituted ring vary from 0.05 to 0.12 (Table S20), with low changes of charge densities at the chloro atom (Table S18). It means that the position of the chlorine does not affect the excited state. Also, the values of Δ_{charge} of unsubsituted ring, in all **PY** forms, are similar (0.13, 0.12, and 0.12) as well as for the pyridone ring (–0.19, –0.23, and –0.23) (Table S20). The similar values and the opposite signs of charge densities (Δ_{charge}) were obtained for **HP** forms: –0.15, –0.19, and –0.15 for the unsubsituted rings, and 0.10, 0.07, and 0.10 for pyridine ring (Table S20). The main differences between **HP** and **PY** forms were noticed in following: in the **PY** form, the unsubsituted ring gains, while the pyridine ring loses electron density. The opposite is true for the **HP** form, with notification that magnitude of electronic density change at the unsubsituted ring atoms is negligible. The noticeable differences are found for the pyridone/pyridine ring, where C12 and C14 atoms of the both rings showed slightly larger positive Δ_{charge} value (from 0.1188 to 0.1490 and from 0.1906 to 0.2093 for both forms), and for C13 somewhat larger negative Δ_{charge} values (from –0.2539 to –0.2324). Perhaps the most important difference between the **HP** and the **PY** form was found for Δ_{charge} values for the oxygen atom (O21). In all compounds in the **PY** form, larger negative Δ_{charge} values of –0.2374, –0.2405, and –0.2402 were found, while for the **HP** form significantly lower negative Δ_{charge} valuesof –0.0741, –0.0687, and –0.0669 were noticed (Table S18). Also, for the same compounds, pyridone nitrogen (N17) of **PY** form has negative Δ_{charge} values (–0.0296, –0.0238, and –0.0176), and the opposite result was found for **HP** form (0.0954, 0.0992, and 0.089) (Table S18).

The both forms of nitro-substituted compounds (**7**–**9**) (Table S19) showed opposite behavior compared with compounds **1**–**3**. *S*ubstituted ring was largely populated with electrons in the course of transition to the excited state (Δ_{charge} for the substituted ring varies from +0.64 to +0.97; Table S20). Most of the electron density (from 50 to 66 %) was situated on the nitro group (atoms No. 33, 34, and 35 have a positive value of Δ_{charge}). Also, analysis of the ICT processes of these compounds indicated two kinds of electron transfer: in **HP** forms, both the pyridine and the unsubstituted phenyl rings lose a significant amounts of electron density: –0.65, –0.60, and -0.41 for the pyridine ring, and –0.32, –0.36, and –0.34 for the unsubsituted ring (Table S20). Extent of ICT between the two unsubstituted rings and the substituted one decreases in the order **7-HP** > **8-HP** > **9-HP** (Δ_{charge} are +0.97, +0.96, and +0.75, respectively), and it seems that this order indeed reflects the magnitude of inductive effect of the nitro group. Interestingly, the unsubsituted phenyl ring has similar Δ_{charge} values (Table S20) for all compounds, while Δ_{charge} of the pyridine ring decreases from *ortho*- to *para*-substituted ones.

The second group consists of the compounds in **PY** forms, in which the decrease of the extent of ICT processes with the increased distance between the substituent and pyridone ring (Δ_{charge} of substituted ring are 0.95, 0.76, and 0.64 for the *ortho*-, *meta*- and *para*-positions of nitro group; Δ_{charge} for the pyridine ring are −0.87, −0.72, and −0.60) was observed. This is also an indication of the decreasing contribution of the substituent polar (inductive/field) effect. Lower extents of ICT processes in **PY** form, in comparison with **HP** form, from unsubstituted ring to the rest of the molecule (Δ_{charge} values for unsubsituted ring are around −0.08, −0.04, and −0.04, which is negligible change) were also observed. This behavior can be explained by comparing geometries of both forms: torsional angles between substituted phenyl and pyridone rings are significantly higher in all **PY** forms (Tables S9–S11). In the **PY** structures, the planar angle of two rings significantly deviated from planarity. This does not allow for significant extent of the π-orbitals overlap; so it is reasonable that low ICT between these two rings exist. The **HP** forms, due to more planar conformation, showed larger extent of ICT processes (Fig. S9). This did not hold for *methoxy*-substituted compounds, where small differences in Δ_{charge} between the unsubstituted ring of both **HP** and **PY** forms were observed. Also, in these structures nitrogen (N17) in the pyridone ring of **PY** form has a negative Δ_{charge} value, and the opposite result was found for the **HP** form. This means that the low changes of electron density at this nitrogen exist (in all structures, Δ_{charge} for this nitrogen have a low negative values), while in all **HP** forms, Δ_{charge} for the same atom are positive (Table S19).

Conclusions

Tautomeric equilibria of title compounds were quantitatively analyzed by UV/Vis spectroscopy and theoretical approaches. The results were obtained by stepwise procedure with conclusion that state of equilibrium is determined by a balanced contribution of solvent and structural effect. From the results of the Kamlet–Taft and Catalán correlation analysis, positive value of coefficient *a* indicates better stabilization of the ground of the **PY** form— and the excited state of the **HP** form— while solvent dipolarity and polarizability are the dominant factors influencing the batochromic shift. The contribution of HBD- specific solvent effect on the state of tautomeric equilibrium of the investigated compounds was confirmed in the mixture of THF/NMF. Adjustments of HBD/HBA properties in solvent mixture could control shift of tautomeric equilibrium. The LFER correlation results showed significant influences of the solvent effects on the transmission mode of substituent effects. The positive solvatochromism for both electron-donor- and electron-acceptor-substituted compounds in all solvents, except for compounds **1**, **4**, **5**, **7**, and **8** in DMSO, DMF, and DMAc, was found. Quantum chemical calculations of the optimal geometries of both tautomeric forms were performed using B3LYP functional with 6-311G(d,p) basis set. The inclusion of solvent effects and the TD-DFT calculations demonstrated that substituents, depending on their position on molecules, significantly change the conjugation, and further affect the ICT character of the investigated 2(1*H*)-pyridones. In general, the most important conclusions derived from Bader's analysis could be defined in following: *methoxy* substituent induces ICT, in the excited state, from substituted ring to the other two rings; *nitro* substituent exerts an opposite effect, *i.e.*, induces ICT from the other two rings to substituted one; and the chloro substituent induces negligible ICT process.

Acknowledgments This study was supported by the Ministry of Education, Science and Technological development of the Republic of Serbia (Project 172013).

References

1. Litvinov VP, Krivokolysko SG, Dyachenko VD (1999) Chem Heterocyc Compd 35:509–540
2. Nir E, Muller M, Grace LI, De Vries MS (2002) Chem Phys Lett 355:59–64
3. Dong F, Miller RE (2002) Science 298:1227–1230
4. Choi K-W, Lee J-H, Kim SK (2005) J Am Chem Soc 127:15674–15675
5. Lopez JC, Isabel Pena M, Eugenia Sanz M, Alonso JL (2007) J Chem Phys 126:191103
6. Brunken S, McCarthy MC, Thaddeus P, Godfrey PD, Brown RD (2006) Astron Astrophys 459:317–320
7. Vaquero V, Sanz ME, Lopez JC, Alonso JL (2007) J Phys Chem A 111:3443–3445
8. Schleger HB, Gund P, Fluder EM (1982) J Am Chem Soc 104:5347–5351
9. Forlani L, Cristoni G, Boga C, Todesco PE, Del Vecchio E, Selva S, Monari M (2002) Arkivoc 11:198–215
10. Rawson JM, Winpenny REP (1995) Coordin Chem Rev 139:313–374
11. De Kowalewski DG, Contreras RH, Diez E, Esteban A (2004) Mol Phys 102:2607–2615
12. Millefiori S, Millefiori A (1990) Bull Chem Soc Jpn 63:2981–2984
13. Reichardt C (2003) Solvents and solvent effect in organic chemistry. Wiley-Vch, Weinheim
14. Michelson AZ, Petronico A, Lee JK (2012) J Org Chem 77:1623–1631
15. Chou P-T, Wei C-Y (1997) J Phys Chem B 101:9119–9126
16. Szyc Ł, Guo J, Yang M, Dreyer J, Tolstoy PM, Nibbering ETJ, Czarnik-Matusewicz B, Elsaesser T, Limbach H-H (2010) J Phys Chem A 114:7749–7760
17. Kamlet MJ, Abboud JLM, Abraham MH, Taft RW (1983) J Org Chem 48:2877–2887
18. Marcus Y (1993) Chem Soc Rev 22:409–416
19. Catalán J (2009) J Phys Chem B 113:5951–5960
20. Hansch C, Leo A, Hoekman D (1995) Exploring QSAR: Hydrophobic, Electronic and Steric Constants; ACS Professional Reference Book. American Chemical Society, Washington, DC
21. Antonov L, Stoyanov S (1993) Appl Spectrosc 47:1030–1035
22. Antonov L, Stoyanov S (1995) Anal Chim Acta 314:225–232
23. Barone V, Polimeno A (2007) Chem Soc Rev 36:1724–1731
24. Wiggins P, Williams JAG, Tozer DJ (2009) J Chem Phys 131:091101
25. Tavakol H (2011) Struct Chem 22:1165–1177
26. Kheffache D, Guemmour H, Ouamerali O (2012) Struct Chem 23:1547–1557
27. Marinković AD, Jovanović BŽ, Todorović N, Juranić IO (2009) J Mol Struct 920:90–96
28. Frisch MJ, Trucks GW, Schlegel HB, Scuseria GE, Robb MA, Cheeseman JR, Montgomery JA Jr, Vreven T, Kudin KN, Burant JC, Millam JM, Iyengar SS, Tomasi J, Barone V, Mennucci B, Cossi M, Scalmani G, Rega N, Petersson GA, Nakatsuji H, Hada M, Ehara M, Toyota K, Fukuda R, Hasegawa J, Ishida M, Nakajima T, Honda Y, Kitao O, Nakai H, Klene M, Li X, Knox JE, Hratchian HP, Cross JB, Bakken V, Adamo C, Jaramillo J, Gomperts R, Stratmann RE, Yazyev O, Austin AJ, Cammi R, Pomelli C, Ochterski JW, Ayala PY, Morokuma K, Voth GA, Salvador P, Dannenberg JJ, Zakrzewski VG, Dapprich S, Daniels AD, Strain MC, Farkas O, Malick DK, Rabuck AD, Raghavachari K, Foresman JB, Ortiz JV, Cui Q, Baboul AG, Clifford S, Cioslowski J, Stefanov BB, Liu G, Liashenko A, Piskorz P, Komaromi I, Martin RL, Fox DJ, Keith T, Al-Laham MA, Peng CY, Nanayakkara A, Challacombe M, Gill PMW, Johnson B, Chen W, Wong MW, Gonzalez C, Pople JA (2004) Gaussian 03, Revision C.02. Gaussian, Inc., Wallingford CT
29. Tang W, Sanville E, Henkelman G (2009) J Phys Condens Matter 21:084204–084210
30. Laaksonen L (1992) J Mol Graph 10:33–34
31. Tsuchida N, Yamabe S (2005) J Phys Chem A 109:1974–1980
32. Kolehmainen E, Ośmialowski B, Krygowski TM, Kauppinen R, Nissinen M, Gawinecki R (2000) J Chem Soc Perkin Trans 2:1259–1266
33. Kolehmainen E, Ośmialowski B, Nissinen M, Kauppinen R, Gawinecki R (2000) J Chem Soc Perkin Trans 2:2185–2191

34. Ajaj I, Mijin D, Maslak V, Brković D, Milčić M, Todorović N, Marinković A (2013) Monatsh Chem 144:665–675
35. Baldwin JE, Gilbert KE (1976) J Am Chem Soc 98:8283–8284
36. Angelova SE, Spassova MI, Deneva VV, Rogojerov MI, Antonov LM (2011) Chem Phys Chem 12:1747–1755
37. Iijima T, Jojima E, Antonov L, Stoyanov S, Stoyanova T (1998) Dyes Pigm 37:81–92
38. Antonov L, Fabian WMF, Nedeltcheva D, Kamounah FS (2000) J Chem Soc Perkin Trans 2:1173–1179
39. Antonov L, Nedeltcheva D (1996) Anal Lett 29:2055–2069
40. Petrov V, Antonov L, Ehara H, Harada N (2000) Comput Chem 24:561–569
41. Antonov L, Kawauchi S, Satoh M, Komiyama J (1999) Dyes Pigments 40:163–170